Bioresource Technology 241 (2017) 340–348

Contents lists available at ScienceDirect

Bioresource Technology

journal homepage: www.elsevier.com/locate/biortech

Evaluation of agricultural residues pyrolysis under non-isothermal conditions: Thermal behaviors, kinetics, and thermodynamics

Jianbiao Chen, Yanhong Wang, Xuemei Lang, Xiu'e Ren, Shuanshi Fan *

Key Laboratory of Enhanced Heat Transfer and Energy Conservation, Ministry Education, School of Chemistry and Chemical Engineering, South China University of Technology, Guangzhou 510640, Guangdong, China

HIGHLIGHTS

- Pyrolysis conversion of rape straw (RS) and wheat bran (WB) was characterized by TGA.
- The pyrolysis performance of RS and WB was improved by increasing heating rate.
- Thermodynamic (ΔH, ΔG, ΔS) & kinetic [E, A, f(x)] parameters were gained by TG curves.
- The best kinetic models for pyrolysis of RS and WB were D_2 and $F_{2.7}$, respectively.
- Biomass pyrolysis requires high temperatures and is endothermic and non-spontaneous.

ARTICLE INFO

Article history:
Received 5 April 2017
Received in revised form 5 May 2017
Accepted 6 May 2017
Available online 23 May 2017

Keywords:
Agricultural residues
Pyrolysis
Kinetic models
Master-plots method
Thermodynamic parameters

ABSTRACT

The thermal conversion characteristics, kinetics, and thermodynamics of agricultural residues, rape straw (RS) and wheat bran (WB), were investigated under non-isothermal conditions. TGA experiments showed that the pyrolysis characteristics of RS were quite different from those of WB. As reflected by the comprehensive devolatilization index, when the heating rate increased from 10 to 30 K min^{-1}, the pyrolysis performance of RS and WB were improved 5.27 and 5.96 times, respectively. The kinetic triplets of the main pyrolysis process of agricultural residues were calculated by the Starink method and the integral master-plots method. Kinetic analysis results indicated that the most potential kinetic models for the pyrolysis of RS and WB were D_2 and $F_{2.7}$, respectively. The thermodynamic parameters (ΔH, ΔG, and ΔS) were determined by the activated complex theory. The positive ΔH, positive ΔG, and negative ΔS at characteristic temperatures validated that the pyrolysis of agricultural residues was endothermic and non-spontaneous.

1. Introduction

Along with socio-economic development and population increases, the energy problems have already seeped to each aspect of society. The massive consumption of fossil fuels by humans will eventually threaten their finite resource nature and meanwhile deteriorate ecological environment including global warming and atmospheric pollutions (Hassan et al., 2016; Wu et al., 2014; Xu et al., 2014). These factors have motivated a growing interest in the potential utilization of alternative fuels, among which biomass resources have attracted particular attention for their abundant reserves, wide distribution, ready availability, and CO_2 neutral property (Saidur et al., 2011). Actually, large quantities of agricultural residues are abandoned, if their energy potential are efficiently exploited, that will produce good benefit of society, environment, and economy (Yahya et al., 2015).

China is a great agricultural country, which generates a considerable number of agricultural residues every year, but most of them are irresponsibly discarded (Gai et al., 2013). As two typical residues, rape straw (RS) and wheat bran (WB) are profusely available in China in terms of resource potential. Generally, most of these two residues were directly burned on the farmland by farmers, which caused serious air pollution by releasing CO_2, SO_2, NO_x, particulate matters, and other pollutants. With the continuous improvement and development of environmental laws, extensive and unreasonable treatments for agricultural residues have been strictly prohibited by Chinese government. Moreover, the undesirable properties such as high hygroscopicity, low grindability and nonuniformity for raw agricultural residues have limited their

* Corresponding author.
E-mail address: ssfan@scut.edu.cn (S. Fan).

http://dx.doi.org/10.1016/j.biortech.2017.05.036
0960-8524/

further recycling and unitization as energy resources (Lu et al., 2013). In order to address the environmental problems brought by direct burning, and overcome drawbacks of raw agricultural residues, many researches have been performed to convert agricultural residues into high added value biofuels or chemical feedstocks by various thermochemical conversion (TCC) technologies, such as pyrolysis, liquefaction, and gasification, acquiring solid char, liquid tar or hydrogen rich gas as the target product (Sonobe et al., 2008; Goyal et al., 2008).

Among various approaches of utilizing agricultural residues, interest in pyrolysis has been growing dramatically. As a single technology, pyrolysis can upgrade raw residues for biofuels, or various intermediate compounds for the chemical industry (Song et al., 2014; Yahya et al., 2015; Gollakota et al., 2016). Considering that the pyrolysis conversion of raw agricultural residues into various products has a high dependence on the kinetics and thermodynamics of the thermal decomposition reactions, the accurate kinetic and thermodynamic parameters are necessary for proper design of a pyrolysis process (Xu and Chen, 2013; White et al., 2011). According to related literature (Gai et al., 2013; Worasuwannarak et al., 2007; Ounas et al., 2011; Aboyade et al., 2011), the thermogravimetric analysis (TGA) is usually employed to evaluate the pyrolysis process of agricultural residues, which can be conducted under non-isothermal conditions with a well-defined heating rate. As reported by Gai et al. (2013), the thermal decomposition properties and kinetics of corn straw and rice husk were systematically investigated in a TGA under non-isothermal conditions. The results showed that the pyrolysis characteristic parameters and apparent activation energies of these two agricultural wastes had inconsistent variation trends, which were closely affected by their distinct chemical compositions. A similar appearance has also been reported in the pyrolysis of rice straw, rice husk, and corncob (Worasuwannarak et al., 2007). Despite their elemental compositions were almost the same, the pyrolysis characteristics were obviously distinct due to their differences in the composition of hemicellulose, cellulose, and lignin. As another important agricultural residue, sugar cane bagasse also gained wide concerns, especially on the non-isothermal kinetic analysis. Ounas et al. (2011) have found that the apparent activation energies for the pyrolysis of sugar cane bagasse could be divided into two steps, 168–180 kJ mol^{-1} for hemicellulose decomposition in the conversion range of 10–40% and 231–240 kJ mol^{-1} for cellulose decomposition in the conversion range of 50–80%, respectively. However, Aboyade et al. (2011) obtained different values of 170–225 kJ mol^{-1} in the conversion range of 10–80%, including 200–300 kJ mol^{-1}, 163–245 kJ mol^{-1} and 80–180 kJ mol^{-1} for thermal decomposition of hemicelluloses, cellulose and lignin derived from sugar cane bagasse, respectively. From these researches, it is quite evident that agricultural residues can be treated as one of the most significant and promising renewable energy resources. Up to now, the pyrolysis conversion of various common types of agricultural residues have been done and reported, but few focused on the thermal decomposition of RS and WB, particularly an absence on thermodynamic analysis.

In this article, the thermal behaviors, kinetics, and thermodynamics from the pyrolysis of RS and WB were evaluated by using thermogravimetric analyzer at three different heating rates. On basis of model-free method and integral master-plots method, the kinetic parameters [E, A, and f(x)] of the thermal degradation of RS and WB were discussed. Furthermore, the thermodynamic parameters, namely the changes of enthalpy (ΔH), Gibbs free energy (ΔG), and entropy (ΔS), were estimated at the pyrolysis characteristic temperatures (the initial decomposition temperature T_v, maximum decomposition rate temperature T_p, and terminal decomposition temperature T_f) by the activated complex theory.

2. Materials and methods

2.1. Materials

As two common agricultural residues, rape straw (RS) and wheat bran (WB) were selected to conduct thermogravimetric analysis experiments. Prior to the thermal analysis experiments, the materials were crushed, sieved with a particle size of 180–350 μm, and then dehydrated in a drying oven at 378.0 K for at least 2 h until obtaining a constant weight. To offer some insights into the properties of raw residues, the proximate, ultimate, and biochemical analysis for RS and WB were performed, and the results were presented in Table 1.

2.2. Thermogravimetric analysis

The thermal analysis experiments of RS and WB were carried out in a NETZSCH STA 449C simultaneous thermal analyzer. In order to reduce the mass transfer and heat transfer limitation generated by samples themselves, the initial weight of agricultural residues was maintained at a small value of 8.0 mg. The agricultural residues placed into the crucible of the thermogravimetric analyzer (TGA) were heated up from ambient temperature to 1073 K at the heating rates of 10, 20, and 30 K min^{-1}. An inert atmosphere was produced by the carrier gas of pure nitrogen (N_2, 99.99% purity). The flow rate of N_2 during pyrolysis was maintained at 80 mL min^{-1}. It was high enough to eliminate some secondary reactions. For each test of heating rate, the blank run was carried out for TG baseline correction without material in the crucible. All thermal analysis experiments were repeated at least twice to ensure the reproducibility of experimental results.

2.3. Kinetic and thermodynamic analysis theory

Generally, the kinetic equation is established under isothermal and homogeneous conditions (Mu et al., 2016). However, the thermal degradation process of agricultural residues in this work was a typical non-isothermal and heterogeneous solid-state reaction, which involves complicated chemical reactions and complex physical processes such as mass transfer, heat transfer, and their interactions. For performing the kinetic analysis for thermal degradation process of agricultural residues, the kinetic equation should be modified by changing the reactant concentration (c) into the conversion degree (x, $x = (m_0 - m_t)/(m_0 - m_f)$ where m_0, m_t, and m_f are the initial weight, the weight at reaction time t, and the final weight, respectively) and dividing the non-isothermal process into innumerable isothermal steps (Vyazovkin et al., 2011, 2014; Du et al., 2014).

$$\frac{dc}{dt} = k(T)\cdot f(c) \Rightarrow \frac{dx}{dT}\cdot\frac{dT}{dt} = k(T)\cdot f(x) \quad (1)$$

where dc/dt or dx/dt represents the reaction or conversion rate; f(c) or f(x) is the thermal degradation mechanism function (Chen et al., 2012, 2013); k(T) is the rate constant, and can be expressed by the Arrhenius formula, $k(T) = A\exp(-E/RT)$ where A, E, R, and T are the pre-exponential factor, apparent activation energy, universal gas constant, and absolute temperature, respectively.

When the non-isothermal thermal analysis experiment conducting at the constant heating rate $\beta = dT/dt$, Eq. (1) can be rearranged to the following form:

$$\frac{dx}{dT} = \frac{A}{\beta}\cdot\exp\left(-\frac{E}{RT}\right)\cdot f(x) \quad (2)$$

The integral form of Eq. (2) can be written as:

$$g(x) = \int_0^x \frac{dx}{f(x)} = \frac{A}{\beta}\int_{T_0}^{T}\exp\left(-\frac{E}{RT}\right)dT = \frac{AE}{\beta R}[P(u) - P(u_0)] \quad (3)$$

where $g(x)$ represents the integrated form of the reaction function; $u = E/RT$ and $P(u)$ represents the temperature integral. Based on Eq. (3), diverse kinetic analysis approaches can be developed by substituting disparate empirical equations for $P(u)$ (White et al., 2011; Janković et al., 2009).

2.3.1. Model-free method

Recently, model-free method has been widely used in evaluating the thermal degradation kinetics of various solid materials, such as coal (Tahmasebi et al., 2013), oil shale (Fan et al., 2016), municipal solid waste (Bhavanam and Sastry, 2015), sludge (Chen et al., 2015a, b), or biomass (Zou et al., 2010; Wu et al., 2014), since they can easily give the value of E without assuming the reaction model. And it is also known as the iso-conversional method, because the determination of E obtained is a function of x. As two most common model-free methods, the Kissinger-Akahira-Sunose (KAS) method and the Flynn-Wall-Ozawa (FWO) method could be written by a general expression (Gai et al., 2013).

$$\ln\left(\frac{\beta}{T^{s}}\right) = C_s - \frac{BE}{RT} \tag{4}$$

where disparate s and B will give rise to diverse model-free methods, i.e. the KAS method by $s = 2$, $B = 1$, the FWO method by $s = 0$, $B = 1.0516$. Provided s and B are respectively changed to 1.92 and 1.0008, the accuracy degree of E is much higher than that determined by the KAS and FWO method. This is the Starink method (Starink, 2003; Vyazovkin et al., 2011).

$$\ln\left(\frac{\beta}{T^{1.92}}\right) = \ln\left(\frac{AR^{0.92}}{g(x)E^{0.92}}\right) - 0.312 - 1.0008\frac{E}{RT} \tag{5}$$

The corresponding temperature integral is:

$$P(u) \cong \frac{\exp(-1.0008u - 0.312)}{u^{1.92}} \tag{6}$$

2.3.2. Integral master-plots method

In each thermal analysis test, the thermal degradation reaction rate at ambient temperature T_0 is much slower than that at the maximum degradation temperature. Thus, the value of $P(u_0)$ would be much smaller than $P(u)$. And Eq. (3) can be approximated as (Wu et al., 2014):

$$g(x) = \frac{AE}{\beta R}P(u) \tag{7}$$

For a single-zone thermal decomposition reaction, the kinetic parameters are constant. The suitable reaction function can be acquired to simulate the thermal data by using the predetermined value of E. Employing $x = 0.5$ as a reference, Eq. (7) would be rewritten as:

$$g(0.5) = \frac{AE}{\beta R}P(u_{0.5}) \tag{8}$$

where $g(0.5)$ is the integral function at $x = 0.5$; $u_{0.5} = E/RT_{0.5}$; $T_{0.5}$ is the temperature at $x = 0.5$.

Dividing Eq. (7) by Eq. (8) can give the integral master-plots formula.

$$\frac{g(x)}{g(0.5)} = \frac{P(u)}{P(u_{0.5})} \tag{9}$$

The theoretical master plots can be calculated via drawing $g(x)/g(0.5)$ versus x from various most frequently used kinetic functions $g(x)$ (Chen et al., 2012; 2013). And the experimental master plots can be estimated via describing $P(u)/P(u_{0.5})$ versus x from the thermal data at diverse heating rates. Eq. (9) shows that, for a specified x, the experimental value of $P(u)/P(u_{0.5})$ will be consistent with the theoretical value of $g(x)/g(0.5)$ when a suitable kinetic model is adopted.

2.3.3. Thermodynamic parameters

The thermodynamic parameters of the thermal decomposition process of RS and WB can be determined by the activated complex theory of Eyring (Boonchom and Puttawong, 2010; Vlaev et al., 2008). The general equation gives

$$A = \left(\frac{e\chi k_B T}{h}\right)\exp\left(\frac{\Delta S}{R}\right) \tag{10}$$

where the pre-exponential factor A is the value calculated by the integral master-plots method. e, χ, k_B, and h represent the Neper number, the transition factor, the Boltzmann constant, and the Plank constant, respectively; and T is the characteristic temperature of the pyrolysis. The change of entropy (ΔS) can be obtained by the following formula.

$$\Delta S = R\ln\left(\frac{Ah}{e\chi k_B T}\right) \tag{11}$$

Since

$$\Delta H = E - RT \tag{12}$$

where the apparent activation energy E can be calculated by the Starink method; The change of enthalpy (ΔH) is the state function of a chemical reaction that indicates heat absorbed]TJ424.1(42Tj/F3-518.1

decomposition of RS and WB at disparate heating rates of 10, 20, and 30 K min^{-1} were presented in Figs. 1 and 2, respectively. It was found that the two agricultural residues differed from each other in their TG and DTG profiles. Overall, the thermal decomposition process of WB was later than that of RS. The main reason for this phenomenon is that WB has a lower percentage of devolatilized components compared to RS. As pointed out by Kumar et al. (2008), the weight of residues after the pyrolysis of samples was mainly determined by the total content of fixed carbon and ash. Consequently, the weight of residues from the experiments agreed so well with the proximate analysis of RS and WB. As a whole, the thermal degradation process of RS and WB could be roughly divided into two zones: a slight decrease in the weight of agricultural residues at temperatures below 450.0 K due to dewatering and release of light volatile compounds; a major weight loss started about 450.0 K and ended at 850.0 K where the compounds of hemicellulose, cellulose, lignin and others persistently decomposed. Yang et al. (2007) found that the weight loss temperature ranges of hemicellulose, cellulose, and lignin were 493.2–588.2 K, 588.2–673.2 K, and 433.2–1173.2 K at 10 K min^{-1}, respectively. However, Quan et al (2016) obtained different results including 433.2–643.2 K, 533.2–683.2 K, and from ambient temperature to about 873.2 K for the thermal degradation of hemicelluloses, cellulose and lignin at 20 K min^{-1}, respectively. As shown in Fig. 1, the weight loss rate peaks at about 610.0 K might be attributed to the thermal decomposition of cellulose and lignin. This is because the weight loss rate peak temperatures of samples in this work were located between that of cellulose and lignin (Quan et al., 2016). Since hemicelluloses had an amorphous and random structure, the pyrolysis of hemicelluloses happened at lower temperatures. Compared the thermal degradation characteristics with those of lignocellulosic biomass, it was found that the peak temperatures of DTG profiles were almost identical for the similar chemical compositions (Chen et al., 2015a, 2015b).

As seen from Figs. 1 and 2, the increase in heating rate merely made the TG profiles move towards higher temperatures, but not change the pattern of thermal decomposition of agricultural residues. As for the DTG profiles, with the heating rates increasing, the characteristic temperatures extended to a higher temperature region, and their values increased distinctly. That was because lower heating rate would result in higher heat transfer efficiency during the programmed heating. Therefore, a larger gradient of temperature across the poor heat conductor of agricultural residues would be formed by increasing the heating rate, which finally increased the thermal degradation rate (Zou et al., 2010; Tahmasebi et al., 2013). Moreover, the temperature shifts and the

increase of DTG could also be explained by the Eq. (4). Similar temperature shifts and DTG increases have also been reported in the researches on the thermal degradation of oil-palm biomass (Idris et al., 2012), corn cobs/sugar cane bagasse (Aboyade et al., 2011), corn straw/rice husk (Gai et al., 2013), and other biomass materials at different heating rates.

For further understanding the effect of heating rate on the pyrolysis characteristics of RS and WB, some characteristic parameters were illustrated in Table 2, which can be gained from TG and DTG profiles. T_v, the initial thermal decomposition temperature; T_p, the maximum decomposition rate temperature; $-R_p$, the maximum weight loss rate; $-R_v$, the average weight loss rate; $\Delta T_{1/2}$, the temperature range at half value of $-R_p$; WL, the total weight loss during pyrolysis; WR, the weight of residues after pyrolysis; T_f, the final thermal decomposition temperature; D, the comprehensive devolatilization index, which can be defined as follows (Chen et al., 2012; Chen et al., 2015a, 2015b):

$$D = \frac{(-R_p) \times (-R_v)}{T_v \times T_p \times \Delta T_{1/2}} \quad (14)$$

As shown in Table 2, whether RS or WB, with the heating rate increasing, the characteristic temperatures (T_v, T_p, $\Delta T_{1/2}$, and T_f) of the thermal degradation moved to higher temperatures, the characteristic decomposition rates ($-R_p$ and $-R_v$) obviously increased. As the heating rate rose, the value of WL increased, but the value of WR decreased. The higher WL and lower WR at a higher heating rate could be attributed to shorter residence times in the TGA and less chars generated by the secondary thermal degradation reactions like cracking, re-condensation and re-polymerization. The similar finding has also been reported by Chen et al. (2015a, 2015b) in the research of petrochemical wastewater sludge pyrolysis. When the heating rate went up from 10 to 30 K min^{-1}, the index of D from the thermal degradation of RS and WB increased from 8.55×10^{-7} to 4.51×10^{-6}%^{2} K^{-3} min^{-2}, and 2.55×10^{-7} to 1.52×10^{-6}%^{2} K^{-3} min^{-2}, respectively. With the heating rate increasing, the pyrolysis performance of RS and WB was improved 5.27 and 5.96 times, respectively.

3.2. Kinetic parameters of RS and WB

3.2.1. Calculation of apparent activation energy E

The kinetic analysis of the thermal decomposition of agricultural residues can acquire more information from TGA experiments. A thorough understanding of pyrolysis kinetics is of great importance to provide guidance for designing a safe, efficient, and reasonable pyrolysis process (Zhu et al., 2015; Mu et al., 2016). The main target of this section is to calculate the kinetic triplets, which are apparent activation energy E, apparent pre-exponential factor A, and kinetic model f(x), from the thermal degradation of two agricultural residues.

On the basis of the recommendation from the Kinetics Committee of the International Confederation for Thermal Analysis and Calorimetry (ICTAC Kinetics Committee), the E values determined by the model-free method should be in a broad x interval of 5–95% with an increment of not greater than 5% (Vyazovkin et al., 2011). However, the initiation and the termination of solid-state reactions are unstable, so the interval of x applied in this article was the middle of 20–80% with an increment of 5% (Janković et al., 2009).

Based on Eq. (5), for a specified x, the E value can be estimated from the slope of regression by plotting $\ln\beta/T^{1.92}$ against 1/T. The plots for the calculation of E using the Starink method at three disparate heating rates of 10, 20, and 30 K min^{-1} were drawn. The approximate parallel regressions reflected that the values of E determined at different x might be described by a single-step reaction mechanism or unification of multiple reaction mechanisms (Li et al., 2015b). The values of slope, E, and correlation coefficient (R^2) for the thermal degradation of RS and WB were calculated and presented in Table 3. Data of R^2 listed in Table 3 were in the range of 0.9897–0.9999, indicating that the E values calculated by the Starink method were very reliable. As suggested by Boonchom and Puttawong (2010), if the relative error of the slope of the straight lines is lower than 10%, it is considered that the E values are independent of x. The values of E presented in Table 3 varied little with x, so the thermal degradation of RS and WB followed a single-step reaction. The average values of E for the pyrolysis of RS and WB were 98.93 kJ mol^{-1} and 96.85 kJ mol^{-1}, respectively. The values could be used in the master-plots method to find the reaction model. In the previous research (Gai et al., 2013), the E values in the conversion (x) range of 0.20–0.80 were 98.72–148.06 kJ mol^{-1} and 50.49–88.99 kJ mol^{-1} for the thermal degradation of corn straw and rice husk, respectively. Aboyade et al. (2011) have reported that the E values in the conversion (x) range of 0.10–0.80 were ranged from 170–225 kJ mol^{-1} to 75–130 kJ mol^{-1} for sugar cane bagasse and corn cobs, respectively. The differences in E values could be ascribed to the biomass sources (species,

Table 2
Pyrolysis characteristic parameters for RS and WB at 10, 20, and 30 K min^{-1}.[1]

Samples	β[a] K min^{-1}	T_v[b] K	T_p[c] K	$-R_p$[d] % min^{-1}	$\Delta T_{1/2}$[e] K	$-R_v$[f] % min^{-1}	WL[g] %	WR[h] %	T_f[i] K	D[j] %^{2} K^{-3} min^{-2}
RS										
	10	435.2	605.6	6.90	86.0	2.81	60.70	24.30	651.2	8.55×10^{-7}
	20	449.4	615.4	12.62	92.0	4.67	62.18	22.06	717.8	2.32×10^{-6}
	30	458.0	626.4	19.29	92.4	6.19	66.79	22.64	790.2	4.51×10^{-6}
WB										
	10	441.4	601.2	4.04	117.2	1.97	53.08	28.36	711.0	2.55×10^{-7}
	20	454.6	616.2	8.16	118.6	3.55	56.98	28.29	777.0	8.72×10^{-7}
	30	457.8	622.8	11.60	135.4	5.06	59.15	26.23	817.0	1.52×10^{-6}

[a] β, the heating rate.
[b] T_v, the initial decomposition temperature.
[c] T_p, the maximum decomposition rate temperature.
[d] $-R_p$, the maximum weight loss rate.
[e] $\Delta T_{1/2}$, the temperature range at half value of $-R_p$.
[f] $-R_p$, the average weight loss rate.
[g] WL, the weight loss of samples during the pyrolysis.
[h] WR, the residual weight after pyrolysis experiment.
[i] T_f, the terminal decomposition temperature.
[j] D, the comprehensive devolatilization index.

Table 3
Slope, activation energy (E), and correlation coefficient (R^2) obtained by Starink method of the pyrolysis of RS and WB.

Samples	x/%	Slope	E/kJ mol^{-1}	R^2	Sample	x/%	Slope	E/kJ mol^{-1}	R^2
RS	0.20	−12.700	105.51	0.9915	WB	0.20	−11.852	98.46	0.9993
	0.25	−12.429	103.26	0.9910		0.25	−11.474	95.32	0.9977
	0.30	−12.244	101.72	0.9945		0.30	−11.559	96.03	0.9983
	0.35	−12.133	100.80	0.9975		0.35	−11.887	98.76	0.9996
	0.40	−12.102	100.54	0.9991		0.40	−12.098	100.51	0.9998
	0.45	−12.035	99.99	0.9999		0.45	−12.369	102.76	0.9999
	0.50	−12.022	99.88	0.9993		0.50	-12.420	103.18	0.9999
	0.55	−12.007	99.75	0.9977		0.55	−12.470	103.60	0.9997
	0.60	−11.878	98.68	0.9948		0.60	−12.259	101.85	0.9992
	0.65	−11.717	97.34	0.9897		0.65	−11.832	98.30	0.9985
	0.70	−11.724	97.40	0.9986		0.70	−11.191	92.97	0.9988
	0.75	−11.148	92.62	0.9915		0.75	−10.486	87.12	0.9999
	0.80	−10.664	88.59	0.9973		0.80	−9.658	80.24	0.9992
Average			98.93					96.85	

producing area, processing mode), operating conditions (particle size, initial sample weight, and heating rate, etc.), and the method used to calculate the kinetic parameters.

3.2.2. Determination of reaction model f(x)

As elaborated in Section 2.3.2, the reaction model of solid-phase reactions could be obtained using the master-plots method. Using Eq. (6), the temperature integral of the thermal degradation of RS and WB can be calculated as a function of the selected x by the previously estimated activation energy E. After that, the experimental master plots of $P(u)/P(u_{0.5})$ versus x from the thermal data at distinct heating rates of 10, 20, and 30 K min^{-1} could be calculated, which were presented in Fig. 3. The plots of $P(u)/P(u_{0.5})$ versus x from the thermal degradation of RS and WB at diverse heating rates were almost overlapped with each other, indicating that the pyrolysis process of agricultural residues could be described by a single reaction model.

Employing most frequently used g(x) functions, the theoretical master plots of g(x)/g(0.5) versus x were gotten. As depicted in Fig. 3, the experimental master plots from the pyrolysis of RS and WB at disparate heating rates were compared with the theoretical master plots. It can be seen that the plots of $P(u)/P(u_{0.5})$ against x from the pyrolysis of RS coincided with the theoretical master plot D_2. With respect to WB, the plots of $P(u)/P(u_{0.5})$ against x were located between the theoretical master plots F_2 and F_3. It turned out that the reaction models of D_n and F_n, $g(x) = (1-x)\ln(1-x) + x$ and $g(x) = [(1-x)^{1-n} - 1]/(n-1)$, might be the most suitable reaction functions for the description of the pyrolysis process of RS and WB, respectively.

3.2.3. Estimation of pre-exponential factor and kinetic exponent

Eventually, to determine the pre-exponential factor A and kinetic exponent n, the expressions of D_2 and F_n were substituted into Eqs. (7), (15) and (16) can be obtained as:

$$g(x) = \frac{AE}{\beta R} P(u) = (1-x)\ln(1-x) + x \quad (15)$$

$$g(x) = \frac{AE}{\beta R} P(u) = \frac{(1-x)^{1-n} - 1}{n-1} \quad (16)$$

On basis of Eq. (15), the most optimal kinetic exponent n for the thermal decomposition of RS were calculated by plotting $(1-x)\ln(1-x)+x$ versus $10^m \times EP(u)/\beta R$ under linear least square fitting method. With regard to the pyrolysis of WB sample, the most probable kinetic exponent n can be analogously estimated by plotting $[(1-x)^{1-n} - 1]/(n-1)$ versus $10^m \times EP(u)/\beta R$ from Eq. (16).

As illustrated in Fig. 4(a-b), the most optimal values of n for the thermal decomposition of RS and WB at the heating rate of

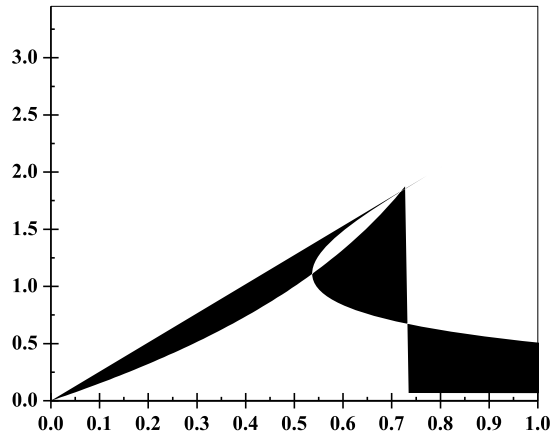

30 K min^{-1} were acquired with the highest correlation coefficient (R^2) and closest zero intercept. Finally, the kinetic triplets (E, A, and f(x)) for the pyrolysis of RS and WB at three diverse heating rates of 10, 20, and 30 K min^{-1} were given in Table 4. To validate the exactness of above kinetic analysis approach, the fit between experimental data and theoretical calculating values was checked.

Based on Eq. (3), the value of x can be calculated as a function of reaction temperature T through using the kinetic parameters in Table 4. As seen from Fig. 4(c-d), the calculated line and experimental data were almost coincident, which indicated that the kinetic triplets can accurately predict and reproduce the thermal degradation process of RS and WB.

3.3. Thermodynamic parameters of RS and WB

The thermodynamic parameters of the thermal decomposition of agricultural residues were of great importance to properly design a reactor in the large-scale pyrolysis process (Xu and Chen, 2013). Table 5 showed the thermodynamic parameters (the changes of enthalpy ΔH, Gibbs free energy ΔG, and entropy ΔS) from the pyrolysis of RS and WB at T_v, T_p, and T_f of 10 K min^{-1}. The positive values of ΔH at the characteristic temperatures reflected that the thermal degradation of RS and WB was an endothermic reaction, meaning that an external source of heat was required to transform the reagents into their transition state (Boonchom and Puttawong, 2010). It is clearly observed that ΔH for RS was slightly larger than that for WB. As for RS, the value of ΔH slightly decreased from 95.31 kJ mol^{-1} to 93.52 kJ mol^{-1} as the pyrolysis temperature went up from T_v, to T_f. Similarly, when the pyrolysis temperature increased from T_v, to T_f, the value of ΔH for WB decreased from 93.18 kJ mol^{-1} to 90.94 kJ mol^{-1}.

The thermal degradation of agricultural residues occurred at T_v was mainly attributed to the evaporation of moisture and light volatile components. With the pyrolysis temperature increasing, the chemical bonds began to break. The parameter of ΔG reflects the increase in total energy of the system at the approach of the reagents and the formation of activated complex (Li et al., 2015a, b). And the value of ΔS is the measure of disorder or randomness of energy and matter in a system (Xu and Chen, 2013). As presented in Table 5, the positive ΔG and negative ΔS at T_v, T_p, and T_f validated that the thermal degradation of agricultural residues was a non-spontaneous process. The values of ΔG for the thermal decomposition of RS were slightly larger than those of WB, which meant that the pyrolysis process of RS needed introducing more heat. The absolute values of ΔS for the pyrolysis of RS were 144.20, 146.95, and 147.55 J mol^{-1} s^{-1} at T_v, T_p, and T_f, respectively. With regard to the pyrolysis of WB, corresponding absolute values of ΔS at T_v, T_p, and T_f were 131.40, 133.97, and 135.36 J mol^{-1} s^{-1}, respectively. Since the absolute values of ΔS from the thermal degradation of RS were slightly higher than those from the pyrolysis of WB, more energy was required for RS to reduce the disorder degree (Li et al., 2015a, b). Furthermore, the low value of ΔS revealed that the samples have just passed through some physical or chemical aging processes, transforming them to a state that was close to their own thermodynamic equilibrium (Huang et al., 2016). As listed in Table 5, whether RS or WB, with the thermal degradation deeply going, the values of ΔS became lower and lower. The results indicated that the state of samples were near their thermodynamic equilibrium. In this situation, the reactivity of thermal degradation of agricultural residues was low, and the

Table 4
Kinetic triplets of the pyrolysis of RS and WB at 10, 20, and 30 K min^{-1}.

Samples	β K min^{-1}	E kJ mol^{-1}	A s^{-1}	f(x)	R^2
RS	10	98.93	7.240×10^5	$[-\ln(1-x)]^{-1}$	0.9975
	20		6.595×10^5		0.9986
	30		6.873×10^5		0.9964
WB	10	96.85	3.426×10^6	$(1-x)^{2.7}$	0.9969
	20		3.531×10^6		0.9985
	30		3.386×10^6		0.9992

Table 5
Thermodynamic parameters of the pyrolysis of RS and WB at T_v, T_p, and T_f of 10 K min^{-1}.

Samples	T_v K	ΔH kJ mol^{-1}	ΔG kJ mol^{-1}	△S J mol^{-1} K^{-1}	T_p K	ΔH kJ mol^{-1}	ΔG kJ mol^{-1}	△S J mol^{-1} K^{-1}	T_f K	ΔH kJ mol^{-1}	ΔG kJ mol^{-1}	△S J mol^{-1} K^{-1}
RS	435.2	95.31	158.07	−144.20	605.6	93.89	182.89	−146.95	651.2	93.52	189.60	−147.55
WB	441.4	93.18	151.18	−131.40	601.2	91.85	172.39	−133.97	711.0	90.94	187.18	−135.36

system needed introducing an external energy source to produce the activated complex. These thermodynamic parameters were consistent with thermal analysis results.

4. Conclusions

The pyrolysis process of rape straw (RS) and wheat bran (WB) could be roughly distinguished as: dewatering and decomposition of volatiles. The pyrolysis characteristics were closely related to chemical components and experimental conditions. Kinetics analysis indicated that the average activation energies for the pyrolysis of RS and WB were 98.93 kJ mol^{-1} and 96.85 kJ mol^{-1}, respectively. The most optimal kinetic models for the pyrolysis of RS and WB were $[-\ln(1-x)]^{-1}$ and $(1-x)^{2.7}$, respectively. The positive ΔH, positive ΔG, and negative ΔS at characteristic temperatures validated that the pyrolysis of agricultural residues was endothermic and non-spontaneous.

Conflict of interest

The authors declare no competing financial interest.

Acknowledgement

Grateful acknowledgement is made to associate Professor Lin Mu and my Ph.D. advisor Professor Hongchao Yin whose constructive comments have helped to improve the quality of this paper. Financial support for this work that has been provided by the Fundamental Research Funds for the Central Universities (2017BQ062) is also gratefully acknowledged.

Appendix A. Supplementary data

Supplementary data (Most frequently used kinetic functions g(x) and plots for calculation of E values by Starink method at different x) associated with this article can be found, in the online version, at http://dx.doi.org/10.1016/j.biortech.2017.05.036.

References

Aboyade, A.O., Hugo, T.J., Carrier, M., Meyer, E.L., Stahl, R., Knoetze, J.H., Görgens, J.F., 2011. Non-isothermal kinetic analysis of the devolatilization of corn cobs and sugar cane bagasse in an inert atmosphere. Thermochim. Acta 517, 81–89.
Bhavanam, A., Sastry, R.C., 2015. Kinetic study of solid waste pyrolysis using distributed activation energy model. Bioresour. Technol. 178, 126–131.
Boonchom, B., Puttawong, S., 2010. Thermodynamics and kinetics of the dehydration reaction of $FePO_4 \cdot 2H_2O$. Phys. B 405, 2350–2355.
Chen, C., Ma, X., He, Y., 2012. Co-pyrolysis characteristics of microalgae Chlorella vulgaris and coal through TGA. Bioresour. Technol. 117, 264–273.
Chen, C., Lu, Z., Ma, X., Long, J., Peng, Y., Hu, L., Lu, Q., 2013. Oxy-fuel combustion characteristics and kinetics of microalgae Chlorella vulgaris by thermogravimetric analysis. Bioresour. Technol. 144, 563–571.
Chen, J., Mu, L., Jiang, B., Yin, H., Song, X., Li, A., 2015a. TG/DSC-FTIR and Py-GC investigation on pyrolysis characteristics of petrochemical wastewater sludge. Bioresour. Technol. 192, 1–10.
Chen, Z., Hu, M., Zhu, X., Guo, D., Liu, S., Hu, Z., Xiao, B., Wang, J., Laghari, M., 2015b. Characteristics and kinetic study on pyrolysis of five lignocellulosic biomass via thermogravimetric analysis. Bioresour. Technol. 192, 441–450.
Du, Y., Jiang, X., Lv, G., Ma, X., Jin, Y., Wang, F., Chi, Y., Yan, J., 2014. Thermal behavior and kinetics of bio-ferment residue/coal blends during co-pyrolysis. Energy Convers. Manage. 88, 459–463.
Fan, Y., Yu, Z., Fang, S., Lin, Y., Lin, Y., Liao, Y., Ma, X., 2016. Investigation on the co-combustion of oil shale and municipal solid waste by using thermogravimetric analysis. Energy Convers. Manage. 117, 367–374.
Gai, C., Dong, Y., Zhang, T., 2013. The kinetic analysis of the pyrolysis of agricultural residue under non-isothermal conditions. Bioresour. Technol. 127, 298–305.
Gollakota, A.R., Reddy, M., Subramanyam, M.D., Kishore, N., 2016. A review on the upgradation techniques of pyrolysis oil. Renewable Sustainable Energy Rev. 58, 1543–1568.
Goyal, H.B., Seal, D., Saxena, R.C., 2008. Bio-fuels from thermochemical conversion of renewable resources: a review. Renewable Sustainable Energy Rev. 12, 504–517.
Hassan, H., Lim, J.K., Hameed, B.H., 2016. Recent progress on biomass co-pyrolysis conversion into high-quality bio-oil. Bioresour. Technol. 221, 645–655.
Huang, L., Liu, J., He, Y., Sun, S., Chen, J., Sun, J., Chang, K., Kuo, J., Ning, X., 2016. Thermodynamics and kinetics parameters of co-combustion between sewage sludge and water hyacinth in CO_2/O_2 atmosphere as biomass to solid biofuel. Bioresour. Technol. 218, 631–642.
Idris, S.S., Rahman, N.A., Ismail, K., 2012. Combustion characteristics of Malaysian oil palm biomass, sub-bituminous coal and their respective blends via thermogravimetric analysis (TGA). Bioresour. Technol. 123, 581–591.
Janković, B., Mentus, S., Jelić, D., 2009. A kinetic study of non-isothermal decomposition process of anhydrous nickel nitrate under air atmosphere. Phys. B 404, 2263–2269.
Kumar, A., Wang, L., Dzenis, Y.A., Jones, D.D., Hanna, M.A., 2008. Thermogravimetric characterization of corn stover as gasification and pyrolysis feedstock. Biomass Bioenergy 32, 460–467.
Li, H., Niu, S., Lu, C., Wang, Y., 2015a. Comprehensive investigation of the thermal degradation characteristics of biodiesel and its feedstock oil through TGA–FTIR. Energy Fuels 29, 5145–5153.
Li, H., Niu, S.L., Lu, C.M., Cheng, S.Q., 2015b. Comparative evaluation of thermal degradation for biodiesels derived from various feedstocks through transesterification. Energy Convers. Manage. 98, 81–88.
Lu, K.M., Lee, W.J., Chen, W.H., Lin, T.C., 2013. Thermogravimetric analysis and kinetics of co-pyrolysis of raw/torrefied wood and coal blends. Appl. Energy 105, 57–65.
Mu, L., Chen, J., Yao, P., Zhou, D., Zhao, L., Yin, H., 2016. Evaluation of co-pyrolysis petrochemical wastewater sludge with lignite in a thermogravimetric analyzer and a packed-bed reactor: pyrolysis characteristics, kinetics, and products analysis. Bioresour. Technol. 221, 147–156.
Ounas, A., Aboulkas, A., Bacaoui, A., Yaacoubi, A., 2011. Pyrolysis of olive residue and sugar cane bagasse: non-isothermal thermogravimetric kinetic analysis. Bioresour. Technol. 102, 11234–11238.